energies

MDPI

Article

Applying Artificial Neural Networks and Nonlinear Optimization Techniques to Fault Location in Transmission Lines—Statistical Analysis

Simone A. Rocha [1,*], Thiago G. Mattos [1], Rodrigo T. N. Cardoso [1] and Eduardo G. Silveira [2]

[1] Program in Mathematical and Computational Modeling, Federal Center for Technological Education of Minas Gerais, Belo Horizonte 30180-001, Brazil; tgmattos@cefetmg.br (T.G.M.); rodrigocardoso@cefetmg.br (R.T.N.C.)

[2] Department of Electrical Engineering, Federal Center for Technological Education of Minas Gerais, Belo Horizonte 30180-001, Brazil; eduardo@cefetmg.br

* Correspondence: simonerocha.025@gmail.com; Tel.: +55-31-992168401 or +55-31-992168402

Abstract: This study presents applications of artificial neural networks and nonlinear optimization techniques for fault location in transmission lines using simulated data in an electromagnetic transient program and actual data occurring in transmission lines. The localization is performed by a modular structure of 4 neural networks and by the minimization of objective functions descriptive of the problem, defined according to the parameters of the line and the type of short circuit, submitted to the methods Quasi-Newton, Ellipsoidal, and Real Polarized Genetic Algorithm. The results obtained are compared statistically with those of a classical analytical method. The analysis of the variance of location errors presented by the methods revealed, with 5% significance, statistical evidence that allowed the conclusion that the type of method used affects fault location indication. In simulated scenarios, minor errors were obtained with the neural network and larger with the analytical method. For field oscillographic, the largest errors were in the neural network; there is no evidence to reject the equality between the results of the analytical method and the nonlinear optimization techniques. The Tukey test identified no differences between the nonlinear optimization methods applied to the proposed objective functions, but the low computational cost associated with the Quasi-newton method highlights it. The nonlinear optimization methods used for the localization function proved to be promising for application in companies that operate electrical systems, providing localization errors similar to those presented by the classical analytical method.

Keywords: fault location; transmission line; artificial neural network; nonlinear optimization; statistical analysis

Citation: Rocha, S.A.; Mattos, T.G.; Cardoso, R.T.N.; Silveira, E.G. Applying Artificial Neural Networks and Nonlinear Optimization Techniques to Fault Location in Transmission Lines—Statistical Analysis. *Energies* **2022**, *15*, 4095. https://doi.org/10.3390/en15114095

Academic Editors: Ioana-Gabriela Sirbu and Lucian Mandache

Received: 2 April 2022
Accepted: 24 May 2022
Published: 2 June 2022

1. Introduction

Overhead transmission lines (TL) are integral components of an electric power system that enable the supply of electric energy from its generation to the distribution networks. Generally, a short circuit (fault) in a transmission line represents a phenomenon that is difficult to predict, and such faults are characterized by the instant of occurrence, the type classification: phase-to-ground (SPG), two-phase (DP), two-phase-to-ground (DPG), or three-phase (TP), the location indication (d_F), and the fault resistance value (R_F). In the event of a fault, the protection relay detects, identifies, and signals the event, commanding the circuit breakers to remove the short-circuited line from service. Following its actuation, automatic restart attempts are made. If successful, the line is reintegrated into the system; however, if the attempts fail, the line needs to be shut down until repair work is performed, which should ideally take place in the shortest time possible and with adequate reliability. Therefore, indicating the point of occurrence of the defect with the most minor possible error reduces the costs related to the shutdown.

Since the 1970s, there has been ongoing research about locating faults in transmission lines. However, it remains a considerable problem. The development of hardware has allowed access to more measurement points with time synchronization via the global positioning system (GPS), creating the possibility of applying new mathematical techniques to problems involving the electric power system. In addition to avoiding the payment of hefty fines to which electricity concessionaires are subject to regulatory agents, locating faults rapidly and accurately directly reflects the quality of the electricity supply and the stability of the system. To address the problem, according to the proposed location method, scholars on the subject establish, as shown in Table 1, the location scenario, the origin and type of signal used, and the characteristics related to the pre-processing of the data. Existing methods typically use phasors of the voltages and currents of the transmission line terminals. Some authors applied the wavelet transform to the sampled signals to extract the detail coefficients and then the energy or frequencies.

Table 1. Signal characterization and preprocessing.

Signals		**References**
Scenario	Simulated	[1–27].
	Simulated and Real	[28–31].
Origin	One Terminal	[1–30].
	Two Terminals/PMUs	[3,7,13,14,18–21,31].
Sign	Current	[14,17,23].
	Voltage	[19].
	Current and Voltage	[1–16].
Pre-processing	Phasors/Discrete Fourier Transform/Least Squares	[1,3,5–11,18,22,24,26,28,30,31].
	Frequency Spectrum/Discrete Fourier Transform/Least Squares	[2,17,27,30].
	Energy/detail coefficient of the Discrete Wavelet Transform	[4,12–16,19].
	Time signals	[15,21,23,25,29].

Several authors have addressed the issue of fault location in TL through artificial neural networks (ANN). In [21], the authors compare these structures to a black box. According to [7], there is no single neural network structure and the results obtained with the technique highlight the possibilities presented by researchers, a situation verified through the bibliographic survey, as shown in Table 2. Multilayer perceptron feedforward networks are predominantly used, with supervised learning backpropagation and the Levenberg Marquardt training algorithm. In most existing studies, with variations among the authors, the training data were obtained by simulating faults along the transmission line, with different values of R_F, fault incidence angle, and equivalent impedance of the sources generated through electromagnetic transient programs. Modular networks, such as those used by [2,5,8,9,12,14,16,17,26,29–31], represent a possibility in solving the problem of locating different types of faults in LTs, contributing to the reduction of computational effort.

Table 2. Characterization of ANN in fault location studies.

ANN		**References**
Model	Multi Layer Perceptron	[1–7,9,11–14,18,19,23,25–27,29–31].
	Others	[3,12,16,20].
Feeding	Feedforward	[1,2,4,7–9,13,14,17,18,25–31].
Learning	Backpropagation	[1,2,7,9,11,13,14,18,23,25–27,29,31].
Training	Levenberg-Marquardt	[1,2,7,9,13,14,18,19,25–27,29,31].
	Others	[16,23].
Activation Function	Sigmoid	[9,19,27,29].
	Hyperbolic Tangent	[1,13,14,31].
	Logarithmic	[19,25,27].
	Gaussian	[30].

Considering some recent work, in the study presented in [23], instantaneous fault current measurements obtained by simulation are used in modular networks with training guided by Bayesian regularization. Most of these tests in that study indicate the short circuit distance with errors below 0.5% in relation to the simulated location. In [25], location errors in the order of 10^{-5} were achieved by employing the magnitudes of the frequencies of simulated fault voltage and current waves to feed the inputs of a single ANN. Moreover, simulated voltage and current signals from one of the line terminals of the electrical system in Great Britain were used in [26] as input in modular networks, obtaining errors of less than 0.7% in relation to the location of the short circuit. Current and voltage wave frequencies from one of the terminals of a 230 kV and 100 km long transmission line, categorized into 5 groups, were used in [27] as inputs to an ANN for the location of simulated SPG type faults, allowing to achieve errors of less than 0.4% in relation to the location of the fault. From the survey of academic production, there is a predominance of the use of ANN in simulated situations, and the results of an application of ANN to real cases of faults in TL are presented only in [30], where reduced errors were achieved in a transmission line of the electricity supply system in Iran. The situation is related to the difficulty of generalizing ANN, which provides reduced errors in simulated fault location cases, but presents a lack of performance when applied to real cases, indicating the difficulty of making the training data represent the systems of the concessionaires assertively.

Regarding the use of optimization techniques, the Simplex method of linear optimization, Nelder-Mead, was applied by [6] to an objective function to obtain the distance and fault resistance of simulated cases. The Nelder-Mead and Broyden–Fletcher–Goldfarb–Shanno numerical optimization methods were proposed in [10] to locate simulated faults in transmission lines. Harmony Search optimization was presented by [15] to estimate the distance from the substation to the fault point in simulated cases. Different optimization techniques are applied by [21] to estimate the fault location from the minimization of an objective function of a variable. In the authors' analysis, although small localization errors were achieved in all situations, the Teaching Learning Based Optimization technique presented a shorter convergence time to obtain the results. A hybrid model that combines the Relief algorithm (which performs the sequential comparison of the entire database, returning a logical response associated with the operating functionality parameters) with the Transformed Wavelet for fault detection and location is proposed [22]. The implementation of genetic algorithms to the problem of fault location in TL is presented in [28] to compare waveforms from digital fault recorders and simulated waves. The phasors obtained during the fault were used to calculate the fitness value. The results of the proposal were not satisfactory when applied to real faults. In [31], the authors proposed objective functions based on symmetrical components that, applied to simulated and real faults in the Brazilian electrical system and minimized by the ellipsoidal algorithm, provided promising results for using the method in practical situations. In the context presented, this paper aims to:

- to analyze the use of ANN and nonlinear optimization techniques (NLO) in the location of TL faults for simulated and real cases of the Brazilian electric power transmission system;
- to compare the results obtained by the analyzed methods with those provided by the classical analytical method (AM), proposed in [32] and used by some electric utilities in practical applications;
- apply a statistical analysis that allows evaluating the existence of differences between the responses obtained by the methods in the fault location process.

The research proposal is related to evaluating and comparing the errors achieved by the implemented methods so that the possibility of joint use can be verified to improve the fault location process in TL. The application of more than one method can give engineering and maintenance teams confidence in indicating the distance to failure. In practice, inaccurate results drive repair personnel away from the point of failure and reduce confidence in the process. The proposed methods, developed and applied in simulated and real situations of faults in the Brazilian electrical system, allow statistical analysis of the variance and application of the Tukey's test to localization errors, validating the difference between the results achieved by the different methods. Also, considering the bibliographic contribution used, the present study made it possible to verify that:

- in simulated scenarios, smaller localization errors are obtained using ANN and larger using the AM, leaving the NLO techniques with intermediate errors. In real scenarios, different from the situation verified in simulations, greater errors were evidenced with the use of ANN, with no statistical evidence to reject the equality between the fault location performed by the AM and the NLO methods;
- the neural networks implemented in the proposed paper, based on techniques found in the literature, proved to be incompatible for application in companies that operate electrical systems, providing location errors significantly greater than the other methods, far from acceptable in practical situations (up to 5%);
- the Quasi-Newton (QN), Ellipsoidal (EL), and genetic (PRGA) of NLO methods were used in the study. Among them, considering the precision and computational effort, the QN method was the most suitable to be used in field applications, being able to be used together with the AM for the defect location indication.

Notably, for the location methods presented, this study does not intend to evaluate the sensitivity of the algorithms to factors such as current and potential transformer errors, line model, errors inline parameters, synchronization, mutual inductance, transposition, and phasor estimation method. Data are presented in equal conditions to all methods. Accordingly, computer programs containing routines and mathematical techniques necessary to provide the distance to the fault in relation to one of the line terminals were implemented.

Although the paper deals with fault location methods, preventive measures such as transient earth voltage measurement to detect partial discharges [33,34], methods to detect faulty insulators [35,36], AM modulation methods to detect sources of problems in voltage parameters [37,38] and thermography [39] can be adopted to reduce or avoid future problems.

2. Materials and Methods

2.1. Simulated Test System

Consider the three-line model of Figure 1, which represents the electrical system of the faulty transmission line proposed for simulation, where L is the extension of the transmission line, and d_F is the distance from the fault point to Terminal S, which occurs through a fault resistance (R_F).

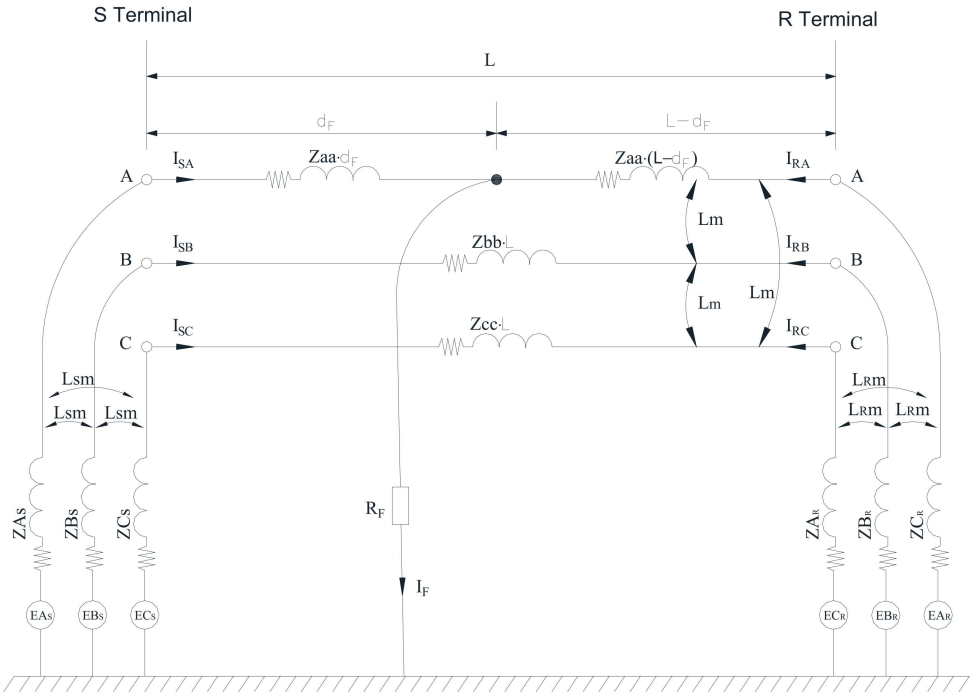

Figure 1. A transmission line with a phase A to ground fault.

The process begins by defining the electrical system used and simulating short circuit cases. A pilot project was developed for a real transmission line of a Brazilian utility that is 74.4 km in length with a capacity of 345 kV. Resistance (r) and reactance (x) data from the terminal equivalent sources and the line are considered to be ideally transposed along its length with lumped parameters, as listed in Table 3.

Table 3. Line parameters and equivalent fonts.

Element	Positive Sequence		Zero Sequence	
	r_1 (Ω)	x_1 (Ω)	r_0 (Ω)	x_0 (Ω)
Line	2.69	27.97	26.94	106.58
Local Source	4.001	34.110	4.069	33.603
Remote Source	6.332	53.845	2.731	39.363

The transmission line parameters were inserted into the Alternative Transients Program (ATP) [40] to obtain simulated data, as shown in Figure 2, where the voltmeter and ammeter represent the protection relay or digital disturbance recorder installed at each line terminal. The simulator contained models of the electrical components of the electrical power system and was used because it is a public domain software. After the simulation, ATP exported a .txt file containing voltage and current data to be used in the various steps that make up fault classification and location programs. The electric energy concessionaire provided only the parameters R, L, and C of the transmission lines used in real case studies. The authors chose to represent the transmission line by resistance and inductance to carry out the studies. More complete models for transmission lines can be used, such as the one by JMARTI [41] and LMARTI [42], as long as the line geometry and cable data are available.

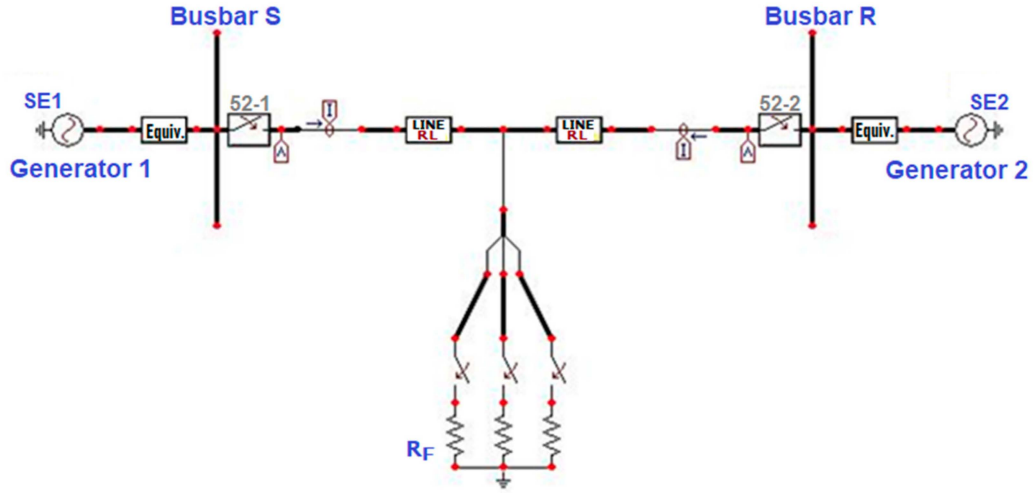

Figure 2. ATP model for short circuit simulation.

From the model, variations in the short circuit location, the R_F value, and the different types of faults were simulated represented in Figure 3: AG—phase A to ground, BG—phase B to ground, CG—phase C to ground, ABG—phase A to phase B to ground, BCG—phase B to phase C to ground, AB—phase A to phase B, BC—phase B to phase C, AC—phase A to phase C and ABC—phase A to phase B to phase C.

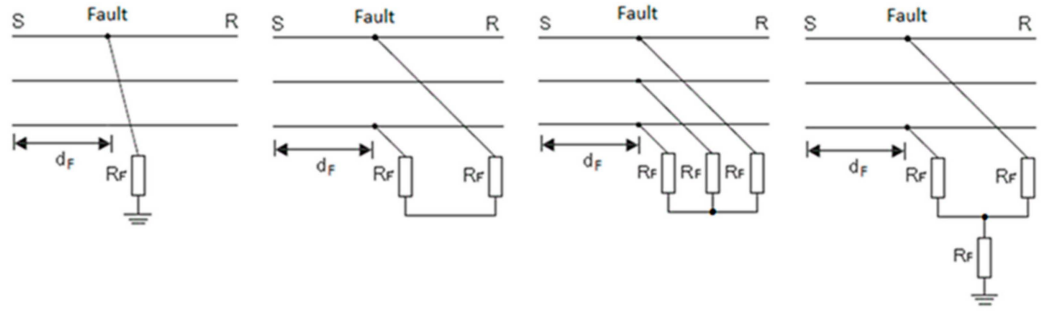

(**a**) (**b**) (**c**) (**d**)

Figure 3. Types of faults: (**a**) SPG (AG, BG, CG); (**b**) DP (AB, AC, BC); (**c**) TP (ABC); (**d**) DPG (ABG, ACG, BCG).

As specified in Tables 4 and 5, the procedure resulted in the generation of 1368 failure scenarios for the composition of the ANN training database and a further 336 cases for the validation of the ANN and application of the three NLO techniques and the AM method. As indicated in [43], the number of training and validation data respectively corresponds to 80% and 20% of the data set. In the case of faults involving the ground, according to references [44,45], higher values of fault resistance can be used to generate data for training neural networks.

Table 4. Composition of fault scenarios: Training of ANN.

	Training Data	**Total**
d_F (km)	Every 5% of the line	19 locations
$R_F(\Omega)$	Cases SPG e DPG: 0-6-12-18-24-30-36-42 Cases DP e TP: 0-1-2-3-4-5	8 values 6 values
Number of scenarios	SPG e DPG: 2·3·8·19 = 912 DP: 3·6·19 = 342 TP: 1·6·19 = 114	1368 scenarios

Table 5. Composition of fault scenarios: validation of ANN, application in NLO techniques and in the analytical method.

	Validation and Application Data	Total
d_F (km)	4-11-17-26-41-53-59-68	8 locations
$R_F(\Omega)$	Cases SPG e DPG: 10-21-26-31-34 Cases DP e TP: 2.5-3.5-4.5	5 values 3 values
Number of scenarios	SPG e DPG: 2·3·8·5 = 240 DP: 3·3·8 = 72 TP: 1·3·8 = 24	336 scenarios

2.2. Process Steps

The necessary procedures involve the steps indicated in the flowchart presented in Figure 4. Data adequacy begins with reading both line terminals' voltage and current inputs. Subsequently, fault detection occurs, which entails the identification of the short circuit start instant in the voltage and current waves, thereby allowing the separation of the data corresponding to the pre-fault and fault periods.

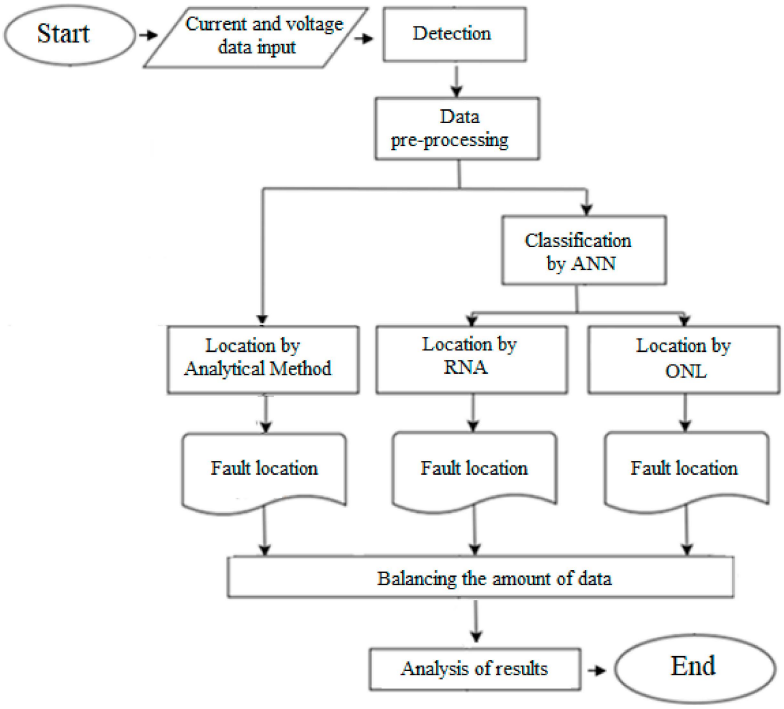

Figure 4. Fault location process.

In the pre-processing of voltage and current signals, necessary for data preparation prior to fault location, higher frequencies were removed by digital low-pass filtering Butterworth with a cut-off frequency of 100 Hz. After that, the sampling frequency was reduced to the desired value of 16 points per cycle of the fundamental frequency (60 Hz in Brazil). The voltages (V_{AS}, V_{BS}, V_{CS}, V_{AR}, V_{BR}, V_{CR}) and currents (I_{AS}, I_{BS}, I_{CS}, I_{AR}, I_{BR}, I_{CR}) phasors associated with the fundamental frequency were estimated through the do least squares method, as described in [46]. Figure 5 shows the voltage and current waves for an AG fault at the sender terminal of the transmission line, which started at 0.049 s. Figure 6 shows the filtered waves, and Figure 7 shows the estimated phasor modules. Figure 8 demonstrates the process of selecting current phasors in phase A. Finally, the fault classification, necessary for the NLO methods, was performed, and then the location process.

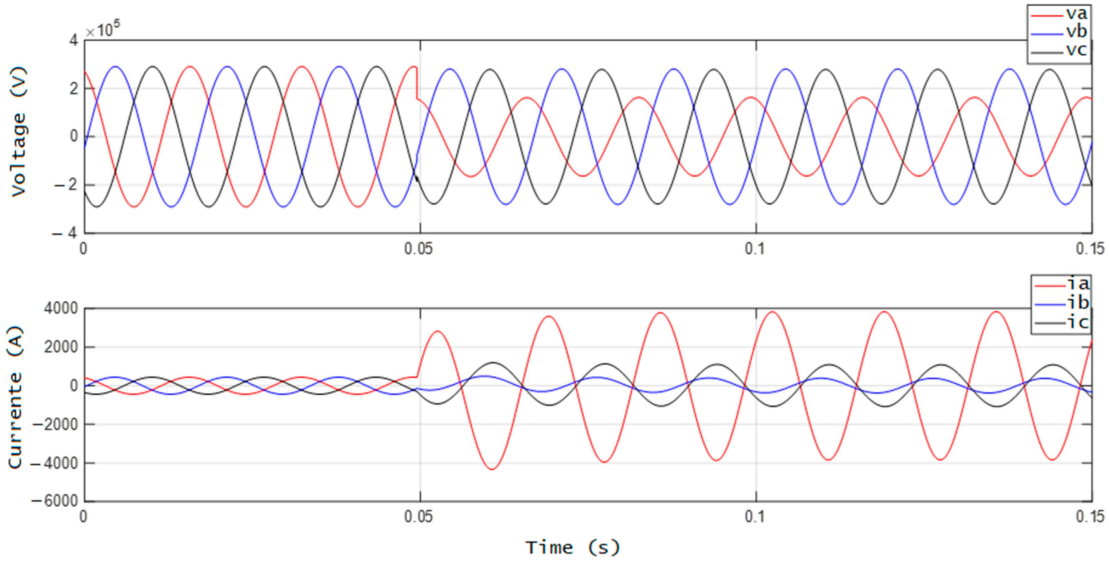

Figure 5. Voltage and current input waves—AG fault.

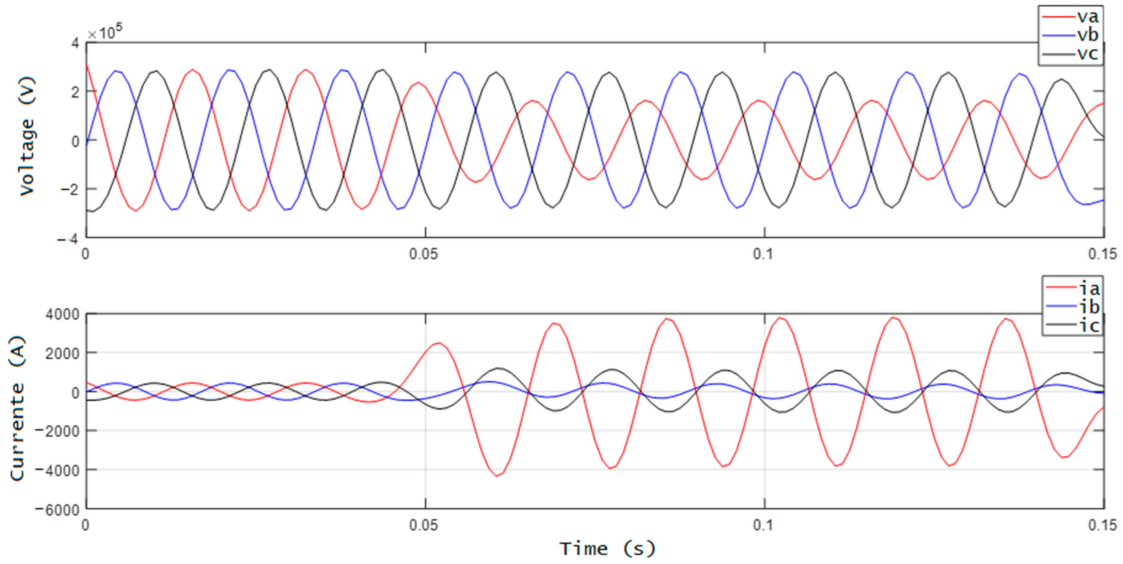

Figure 6. Filtered voltage and current waves—AG fault.

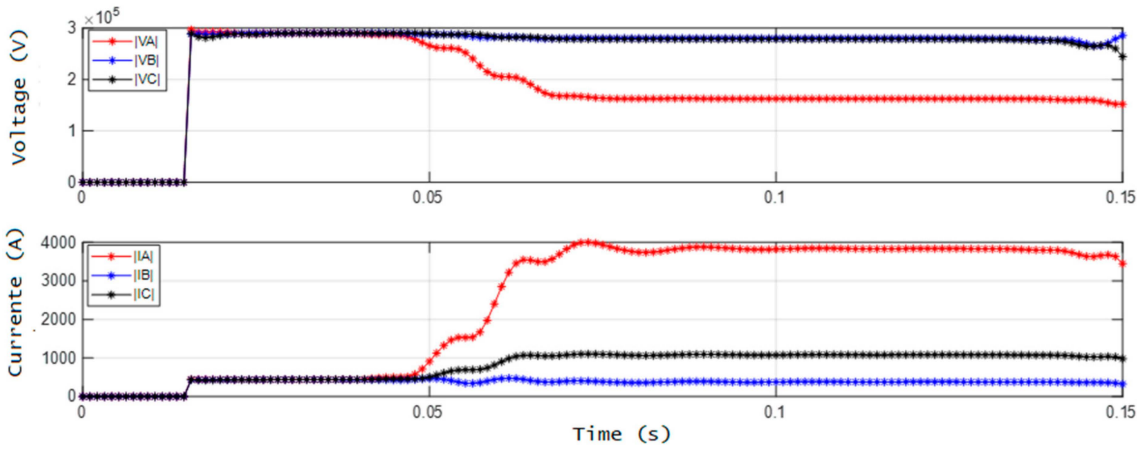

Figure 7. The amplitude of voltage and current phasors—AG fault.

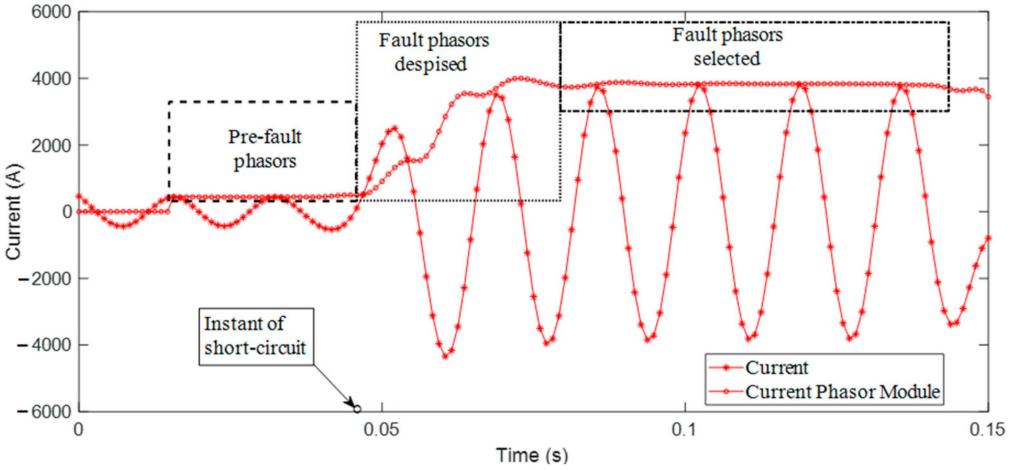

Figure 8. Detail of selection of phasors from the missing phase A current signal, after low-pass filtering.

Fault location occurs after the fault detection and classification steps. In this study, it was estimated through ANN and NLO techniques applied to the objective functions adapted from [31], as well as the analytical method proposed in [32], implemented through MATLAB® software.

2.3. ANN for Fault Location

For fault location, ANN was implemented using the neural network toolbox in MATLAB®, as described by [47]. In structuring the networks, the training was performed separately according to the type of short circuit identified by the classification. Feedforward networks were used with supervised learning backpropagation and the Levenberg-Marquardt training algorithm hyperbolic tangent activation function. In the feedforward model, the network was arranged in layers, and the propagation of information followed from the input to the output without feedback from previous units. The supervised learning backpropagation and Levenberg Marquardt training algorithm were used to minimize the error obtained by the difference between the response in the output layer and the desired value from the correction of the weights in all layers, starting from output to input. The organization of neurons and layers was defined experimentally, with 2 hidden layers of 30 and 20 neurons. After pre-processing the data simulated by ATP, the voltage (V_{AS}, V_{BS}, V_{CS}, V_{AR}, V_{BR}, V_{CR}) and current (I_{AS}, I_{BS}, I_{CS}, I_{AR}, I_{BR}, I_{CR}) phasors amplitude from the local and remote terminals of the line were used as the input data for training the ANN, with the function of providing the estimated fault location as an output, according to the selected modular structure, as indicated in Figure 9.

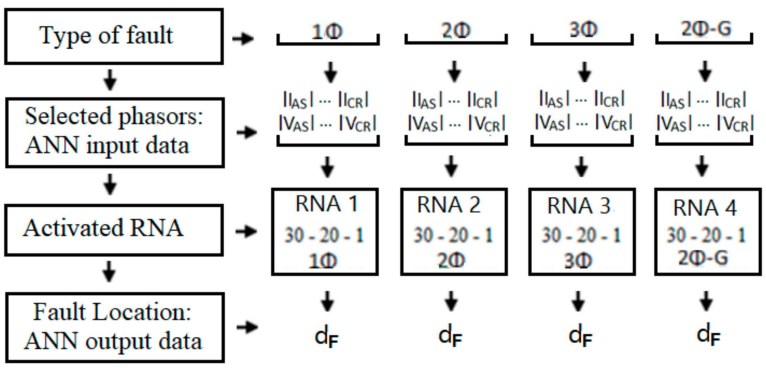

Figure 9. The Modular structure of fault location ANN.

The voltage and current phasors from each validation file in Table 5 were inserted into the trained networks to verify the generalization and adaptation capacity of the location ANN, returning the distance of fault.

2.4. Nonlinear Optimization for Fault Location

The NLO problem used in this study involves minimizing a nonlinear objective function $f : D_f \subset \mathbb{R}^n \rightarrow \mathbb{R}$, overall vectors $x \in D_f$. Depending on the logic employed to determine the solution to the problem, different minimization techniques can be applied to the function f to provide a particular solution $x^* \in D_f \subset \mathbb{R}^n$ such that $\forall\ x \in D_f$, $f(x^*) \leq f(x)$. In this context, the fault location problem is related to the minimization of one of the mono-objective functions, $F(d_F, R_F)$, indicated in Table 6. These functions, adapted from [31], contain fault location and fault resistance as variables, which are based on the currents and voltages of the TL terminals and depend on the types of existing faults. Therefore, the variables must be included in minimization algorithms. The subscripts 0 and 1 indicate, respectively, the values of zero and positive sequence, Z denotes the impedance of the line in Ω/km, I_S, I_R, V_S and V_R denote the respective currents and voltages at the local (S) and remote (R) terminals.

Table 6. Objective functions.

Type of Fault	$F(d_F, R_F)$
AG, BG, CG	$\left\lvert V_S - d_F Z_1 \left(I_S + \left(\frac{Z_0 - Z_1}{Z_1} \right) I_{S0} \right) - 3R_F(I_{S1} + I_{R1}) \right\rvert^2$
AB, BC, CA	$\lvert V_{S1} - V_{S2} - d_F Z_1 (I_{S1} + I_{S2}) - 2R_F(I_{S1} + I_{R1}) \rvert^2$
ABG, BCG, CAG	$\lvert V_{S1} - V_{S0} - d_F Z_1 I_{S1} + d_F Z_0 I_{S0} + 3R_F(I_{S0} + I_{R0}) \rvert^2$
ABC	$\lvert V_{S1} - d_F Z_1 I_{S1} - R_F(I_{S1} + I_{R1}) \rvert^2$

The graphical and analytical analyses of the objective functions that describe the process make it possible to place them as differentiable, convex, and unimodal representations of two real variables, represented by $F(d_F,\ R_F)$. As an example of the characteristics of the function, the graph of a simulated AG fault event occurring 45 km away with R_F of 20 Ω is illustrated in Figure 10. NLO methods based on the search direction and the exclusion of regions and population dynamics were applied to minimize the objective functions. The NLO techniques are primarily distinguished by the logic used in the search for the solution to the problem.

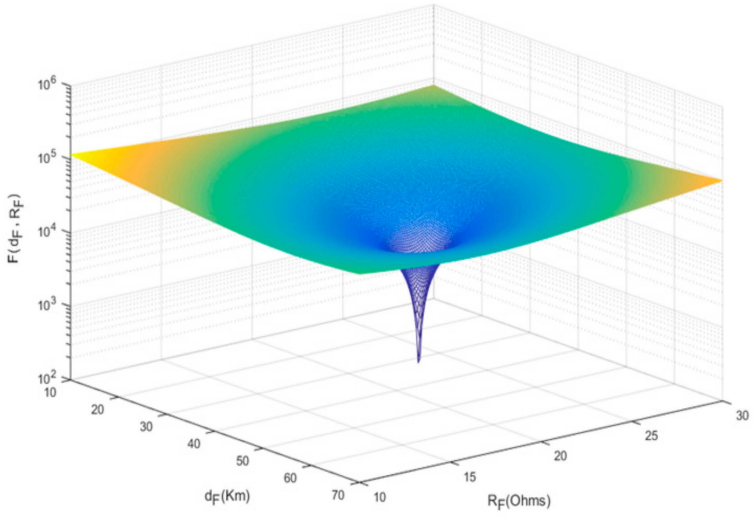

Figure 10. Objective function: fault AG (d_F = 45 km, R_F = 20 Ω).

2.4.1. Search Direction Methods

The Quasi-Newton search direction method used in the research indicates the minimum of the objective function. Information from previous searches is considered until the algorithm satisfies some previously established stopping criterion. From the gradient information, approximations are generated recursively to estimate the inverse of the hessian of the objective function. There are different strategies for this approximation, and, among the methods described by [48], the combination between the DFP (Davidson-Fletcher-Powell) and BFGS (Broyden-Fletcher-Goldfarb-Shanno) methods was used, as indicated in lines 14, 15, and 16 of the algorithm presented in Algorithm 1. The vector r represents the difference between the gradient vector of the objective function in the current position and the previous position; the vector v is the difference between the current position and the previous one, the coefficient γ indicates the weight of DFP and BFGS, and H represents the approximation to the hessian of the objective function.

Algorithm 1 Quasi_Newton Algorithm (y,x)

1 **Start**
2 $n \leftarrow |\, x \,|$
3 $H \leftarrow I_n$
4 $g \leftarrow gradient(x)'$
5 $x_{ant} \leftarrow x$
6 $g_{ant} \leftarrow g$
7 **While** $(set\ stop\ criterion)$
8 $d \leftarrow (-Hg)'$
9 $\alpha \leftarrow one - dimensional(x, d)$
10 $x \leftarrow x_{ant} + \alpha d$
11 $g \leftarrow gradient(x)'$
12 $v \leftarrow (\, x - x_{ant})'$
13 $r \leftarrow g - g_{ant}$
14 $CDFP \leftarrow \dfrac{v\, v'}{v'r} - \dfrac{H\, r\, r'H}{r'\, H\, r}$
15 $CBFGS \leftarrow \left(1 + \dfrac{r'H\, r}{r'v}\right)\dfrac{v\, v'}{v'r} - \dfrac{v\, r'H + Hrv'}{r'v}$
16 $C \leftarrow (1-\gamma)CDFP + \gamma CBFGS$
17 $H \leftarrow H + C$
18 $x_{ant} \leftarrow x$
19 $g_{ant} \leftarrow g$
20 **end**
21 **return**
22 **end**

The search direction methods perform local searches and are strongly dependent on the derivative, the hessian of the objective function, or both at the points obtained at each iteration. Consequently, it may present difficulties for their use. When applied to convex functions, converge to the local minimum, which in these cases also represents the global minimum, a condition verified for the adapted objective functions of [32]. However, if the function were not convex, the local minimum cannot be considered the global minimum. If the objective function were multi-modal, there would be several basins of attraction. Thus, the problem of determining the global minimum would be complex using only local information. This is because of the inability to recognize a global minimum, even within a set of well-defined local minima. The graphic representation shown in Figure 11 exemplifies the sequence of points generated by the QN method for a simulated AG fault at 29.76 km from the transmission line's emitting terminal, with an R_F of 20 Ω.

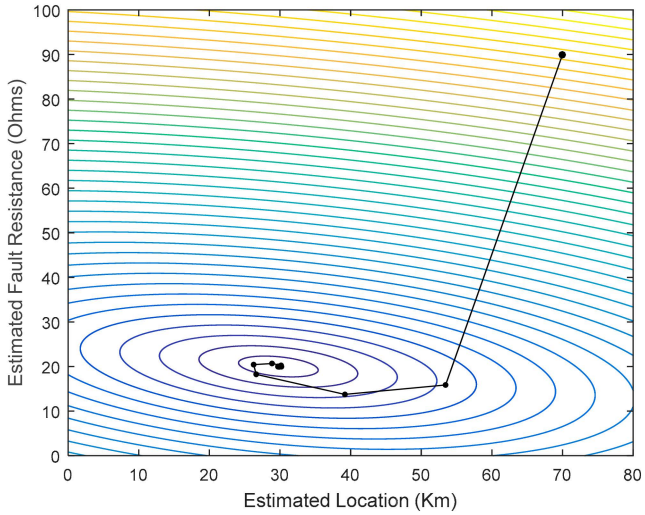

Figure 11. Fault location and resistance: Quasi-Newton.

2.4.2. Region Exclusion Methods

The ellipsoidal method is a region exclusion method. Accordingly, in a convex set with a non-empty interior, the minimum can be found in a finite number of steps through projections in half-spaces and investigation of the subgradients of the objective function. Intuitively, as described in [49], from an initial ellipsoid, which contains the point to be reached, cuts were made to always generate ellipsoids of decreasing volumes for a fixed ratio, which only depends on the dimension of space. The process is outlined by the algorithm shown in Algorithm 2.

Algorithm 2 Ellipsoidal Algorithm (x,Q)

Start
  $n \leftarrow |\, x \,|$
  $\beta_1 = \dfrac{1}{n+1}$
  $\beta_2 = \dfrac{n^2}{n^2-1}$
  $\beta_3 = \frac{2}{n+1}$
  While (*set stop criterion*)
    $m \leftarrow subgradient(f(\cdot), x)$
    $x \leftarrow x - \beta_1 \dfrac{Q_m}{\sqrt{m' Q m}}$
    $Q \leftarrow \beta_2 (Q - \beta_3 \dfrac{(Q_m)(Q_m)'}{m' Q_m}$
  end
  return
end

In the algorithm, n denotes the dimension of the initial point, Q represents the matrix of the ellipse that surrounds the optimal point to be obtained at each iteration, and the vector m_k is the subgradient of the objective function at a given point belonging to the domain of the function. A sequence of points is generated in which x_k represents the center of each ellipsoid. After a finite number of iterations, the smallest ellipsoid over the sought point $x^* \in D_f \subset \mathbb{R}^n$ is obtained such that $\forall\, x \in D_f$, $f(x^*) \leq f(x)$ is given by the center of the ellipsoid. In the Ellipsoidal algorithm, the graph in Figure 12 represents the sequence of points generated by the EL method for the same fault simulated in Figure 11.

At each iteration, the EL method returns the center of the ellipsoid generated in the process. The exclusion of regions occurs from the subgradient without any direct dependence on the derivatives of the objective function. However, the method requires the objective function to be convex or quasi-convex and unimodal, which is also verified with the adapted functions in [31]. If these conditions are not met, it will lead the algorithm to an unpredictable situation.

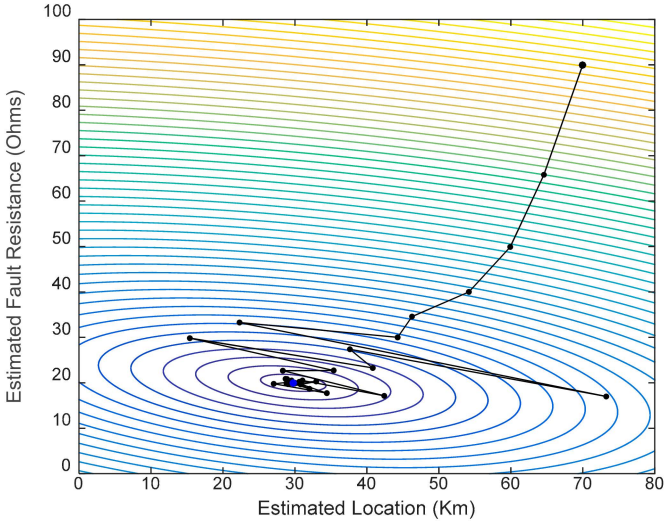

Figure 12. Fault location and resistance: Ellipsoidal.

2.4.3. Population Methods

The search with population methods seeks to reach optimal solutions from a set of solutions. The minimization of a function using a genetic algorithm represented schematically in Algorithm 3 commences from the random generation of a set of points (individuals) that form the initial population studied, representing possible solutions for a given problem. Crossover and mutation genetic operators are applied sequentially during the iterative process, followed by evaluation and selection processes to generate the surviving population. The evaluation of each results in a value called fitness. The better the fitness value, the greater the individual's chance to remain in the surviving population.

Algorithm 3 Genetic Algorithm (x)

```
Start
    P ← Initial population generation ()
    Assessment (P)
    While (set stop criterion)
        P' ← Selection (P)
        P'' ← Crossing (P')
        P'' ← Mutation (P'')
        Evaluation (P'')
        P ← Survivor Population (P ∪ P'')
        Updates (x, P)
    end
    return x
end
```

For the NLO desired in this study, the best fitness is associated with the set of solutions (d_F, R_F) that minimize $f : D_f \subset \mathbb{R}^n \to \mathbb{R}$. The population evolution along the iterations occurs according to an established stopping criterion that leads the set of individuals

to a region close to the optimal point. Population methods do not use information involving derivatives of the objective function for convergence. Instead, they operate with parameter encoding and indicate optimal solutions from a set of solutions. Owing to its non-deterministic character, the process is indicated for the treatment of functions and constraints that are difficult to model, requiring statistical analysis to study their convergence. In this study, we employed the polarized real genetic algorithm described in [50]. In PRGA, each optimization parameter is represented by a real variable, and the set of parameters is stored in a vector that represents an individual. For the simulated AG fault located 29.76 km from the emitting terminal of the transmission line, with an R_F of 20 Ω, the graph presented in Figure 13 refers to the last generation of the PRGA execution.

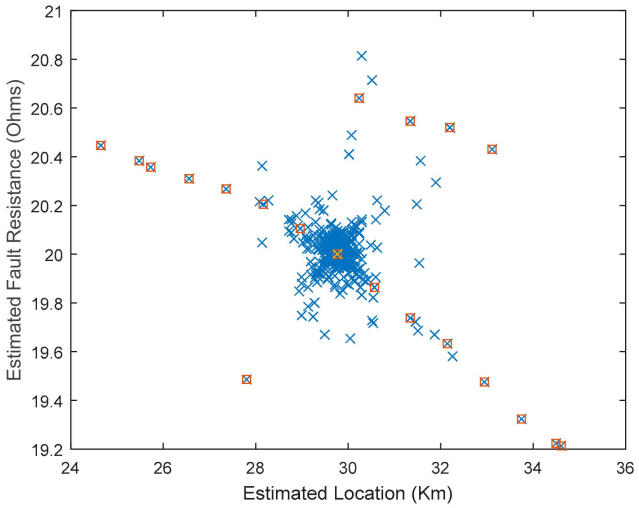

Figure 13. Fault location and resistance: PRGA.

The previously described NLO algorithms were applied to the minimization of the objective functions adapted from [31]. Based on the type of fault, the estimated distance to the point of occurrence of the short circuit in relation to the line terminal was obtained for each of the scenarios specified in Table 5. A variation of the analytical method, which disregards the capacitance of the TL, proposed in [32] was also implemented and applied to the validation cases for comparisons of its results with those provided by the ANN and NLO methods. In this method, fault location is obtained from descriptive functions of the electrical circuit, capable of representing the voltage and current variations along the transmission line from its two terminals.

3. Statistical Study

An analysis of possible statistical differences between the proposed location methods and the types of fault that can occur in a fault event was developed by analyzing the variance with two factors (Anova2) of the location errors presented by the methods using Python [51]. The procedure, as described in [52], allows us to investigate the equality of means in experiments with more than one factor. For the application of the process, the test data must be obtained randomly, and the data must be adjusted to a normal distribution, with mean $\mu = 0$ and constant variance σ^2. These requirements, used in the process of formulating the Anova2 model, allow the generalization of a population from a sample. Regarding the test, it is possible to verify the existence of evidence of variations between the levels of factors that may interfere in the process, signaling the existence of at least one level that differs from the others. In applying the method to the fault location problem, the type of method and the type of fault that occurred were considered factors to be analyzed. Internally, different levels were considered for each of these factors, as shown in Figure 14.

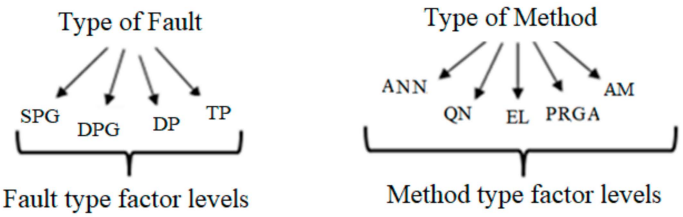

Figure 14. Factors and levels of the location problem.

Mathematically, Anova2 can be expressed using Equation (1), and it is suitable for the problem to be studied. Accordingly, μ is considered as the global average effect of errors arising from the experimental location process, τ_i denotes the effect of the ith level of the fault type factor, β_j represents the effect of the jth level of the method type factor, $(\tau\beta)_{ij}$ indicates the effect of the interaction between the fault type and method type factors, i is the number of levels of the fault type factor, j indicates the number of levels of the method type factor, and k denotes the number of samples collected for each level.

$$y_{ijk} = \mu + \tau_i + \beta_j + (\tau\beta)_{ij} + \varepsilon_{ijk} \begin{cases} i = 1, \ldots, a \\ j = 1, \ldots, b \\ k = 1, 2, \ldots, k \end{cases} \quad (1)$$

The test deals with the influence of the interaction between the two factors analyzed and occurred on the hypothesis tests described in Equations (2)–(4). Each null hypothesis (H_0) supports the assumption that the averages of the errors of the levels are the same for the analyzed factor. Moreover, with the alternative hypothesis (H_1), the existence of at least one different average is assumed. The test results conducted and interpreted in [52] provide tools that allow us to either accept or reject a statistical hypothesis through the evidence provided by the sample.

$$\begin{cases} H_0 : \tau_1 = \ldots = \tau_i = 0; \\ H_1 : \exists\, i / \ \tau_i \neq 0 \end{cases} \quad (2)$$

$$\begin{cases} H_0 : \beta_1 = \ldots = \beta_j = 0; \\ H_1 : \exists\, j / \ \tau_j \neq 0 \end{cases} \quad (3)$$

$$\begin{cases} H_0 : (\tau\beta)_{ij} = 0 \ \forall i, j; \\ H_1 : \exists\, i,\ j / \ (\tau\beta)_{ij} \neq 0 \end{cases} \quad (4)$$

When the Anova2 results reject H_0 and, consequently, accept H_1, there is statistical evidence that at least one of the means of the levels differs from the others for the analyzed factor. This conclusion, analyzed for the fault location problem, allows us to verify whether the type of fault that occurred or the type of method used leads to a differentiation in the efficiency of the location process. The rejection of H_0 is performed by considering a certain level of significance related to the probability of rejecting this hypothesis when it is true. In statistical hypothesis tests, the rejection of H_0 is considered to be significant when the observed p-value is lower than the significance level defined for the study.

Although the Anova2 test indicates the existence of a discrepant level among the others, it does not locate the observed difference. It is necessary to apply a test of comparison of means between the levels to determine the best (or worst) level of the factor. As a complement to the Anova2 study, the Tukey test was applied at a significance level of 5%. The test involves building confidence intervals for all pairs of means in such a manner that the set of all intervals has a certain degree of confidence.

4. Results

In the fault location process, deterministic (QN, EL, AM) and non-deterministic (ANN and PRGA) procedures were implemented and applied. In the application of ANN to the problem, intelligent processes are used to recognize patterns simulated by the ATP related to the identification of the fault location. These structures characterized by adaptation by experiences, learning ability, generalization ability, data organization, etc., can provide a satisfactory solution to the problem. We attempted to obtain the minimum point of an objective function of two variables by applying the implemented NLO algorithms, $f(d_F, R_F)$, from the methods of QN, EL, and PRGA. Table 7 shows the number of iterations performed and the execution time required by each algorithm to reach the result referring to a given fault case.

Table 7. The number of iterations and execution time per method.

Method	ANN	PRGA	QN	EL	AM
Number of iterations	-	42	5	69	-
Time (s)	579	16	0.7	0.8	0.6

4.1. Fault Location: Simulated Cases

The quantities expressed in Table 8 refer to the number of simulated cases for validation of ANN and the application of NLO techniques and the AM method, which depends on the type of fault and the methods implemented. A statistical study is needed to compare the methods used in this study. Owing to the stochastic characteristics of the location by the ANN and by the PRGA, the means and variances of the location values of these methods were obtained from 40 executions.

Table 8. Validation cases by fault type and method.

Type of Method		ANN	PRGA	QN	EL	AM
Type of Fault	DPG	4800	4800	120	120	120
	SPG	4800	4800	120	120	120
	DP	2880	2880	72	72	72
	TP	960	960	24	24	24

Following the implementation and execution of the location step, the balancing of the number of samples per class was applied for the adequacy of the data used. Accordingly, 24 samples were randomly selected from each of the possible combinations of the studied factors, a number corresponding to the smaller quantity of samples of the relationship between the fault event and the implemented methods, as listed in Table 8. Associated with the Anova2 test, the results achieved in the balanced experiment allow the use of the differences between the averages of the levels for the estimates of the main effects of the factors and the interaction between them. When the experiment is unbalanced, differences in factor level means may be associated with unbalanced observations rather than changes in factor levels.

From Equation (5), the percentage errors of the results indicated for each fault location were calculated, provided by the difference between the estimated value by each method and the simulated value in relation to the length of the line.

$$e(\%) = \left| \frac{estimated\ location - simulated\ location}{line\ length} \right| \text{x}100 \quad (5)$$

In simulated scenarios, regardless of the type of fault that occurred, the analysis of the Box-plots of the percentage errors, represented in Figure 15, revealed the better performance of the ANN.

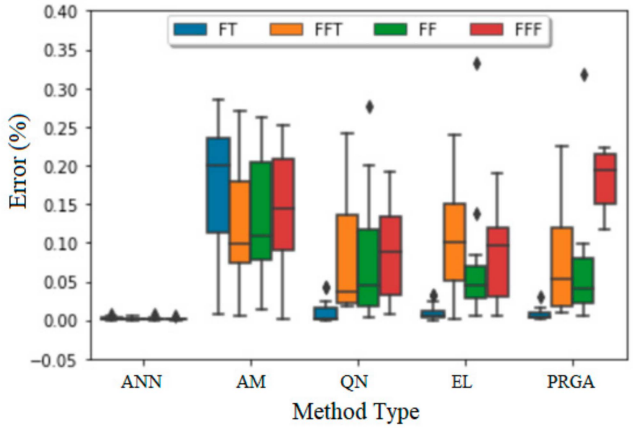

Figure 15. Location errors: simulated cases.

The verification of the existence of differences between the types of methods was based on the Anova2 statistical test. Particularly, considering the results provided by the AM method and the NLO methods, when conducting the analysis of variance for the comparison of samples, it was assumed that the observations were independent and normally distributed, maintaining the variance constant in each treatment. According to [52], the graphic results expressed in Figure 16 made it possible to verify that these assumptions were satisfied.

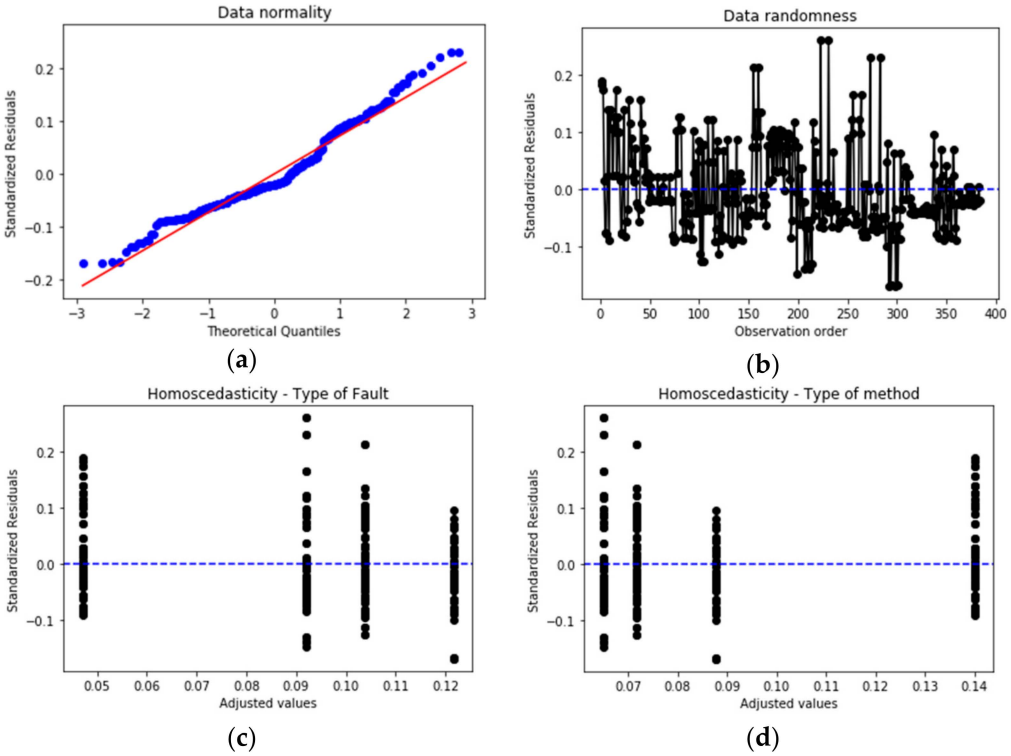

Figure 16. Assumptions for the application of the Anova2 model. (**a**) Data normality; (**b**) Data randomness; (**c**) Homoscedasticity—Type of fault; (**d**) Homoscedasticity—Type of method.

In the quantile-quantile plot of Normal shown in Figure 16a, the configuration of points approached a straight line, indicating that the residuals are normally distributed. The residuals shown in Figure 16b were located approximately around a horizontal band, signaling the validity of the independence assumption. Regarding the homoscedasticity of the levels of the type of fault and type of method factors, Figure 16c,d present the residual plots from randomly arranged points without a set pattern for level change, having adjusted

values both for the type of fault factor and type of method factor. In addition to graphical analysis, the verification of the premises for the application of Anova2 was based on statistical tests, as indicated in [53]. In this sense, the randomness of the residues was verified by applying the Durbin-Watson test (D_W), with the result D_W = 1.805907. The D_W test statistic is in the range between 0 and 4; values close to 2 indicate no correlation between the residues, ensuring the randomness of the sample. The normality of the residues, with 5% significance, was verified by the Shapiro-Wilk hypothesis test (S_W), with a *p*-value result (S_W) = 6.023376×10^{-2}. To test the normal distribution, it is assumed that H_0 is symmetric, whereas H_1 assumes that the variable distribution is asymmetrical. In the Shapiro-Wilk test, the test's significance was greater than 0.050, *p*-value > 0.050, indicating that the residues follow a normal distribution. Regarding the homoscedasticity of the residues, Bartlett's test (B) was used, which is not affected by the sample size and should be used when the residues present normal distribution, and also the Levene test (L), which, although limited to balanced samples, does not require the assumption of normality. In these tests, H_0 indicates that the residue variances are homoscedastic, and H_1 assumes that at least one variance differs from the others. For the type of fault, the tests provided as a result *p*-value (B) = 6.071991×10^{-1}, *p*-value (L) = 3.748992×10^{-1} and for type of method *p*-value (B) = 2.511740×10^{-1}, *p*-value (L) = 5.339021×10^{-2}.

As presented in Table 9, the application of the Anova2 test leads to the rejection of the null hypothesis for both factors analyzed. Specifically, about the location methods evaluated, the indication is that at a 5% significance level, the effects of the type of method affect the percentage error for the fault location, with at least one of the location methods that differ from the others. The result of the *p*-value (PR) obtained by the test statistic was close to 5.816931×10^{-12}, a value considerably lower than 5%. With the data from Table 9, it is also possible to make inferences regarding the types of faults. However, this analysis was not addressed in the proposal of this study.

Table 9. Anova2 testes: simulated cases.

	sum_sq	Df	F	PR(>F)
C(Type_Fault)	0.291482	3.0	17.384073	1.362907×10^{-10}
C(Type_Method)	0.332668	3.0	19.840463	5.816931×10^{-12}
Residual	2.107073	377.0	NaN	NaN

As a complement to the Anova2 study in simulated cases, the Tukey test was applied at a significance level of 5%, and the results expressed in Table 10 were obtained.

Table 10. Multiple comparisons of means: Tukey HSD, FWER = 0.05—simulated cases.

Group1	Group2	Meandiff	Lower	Upper	Reject
PRGA	EL	−0.0162	−0.0457	0.0134	False
PRGA	AM	0.0522	0.0226	0.0818	True
PRGA	QN	−0.0228	−0.0524	0.0068	False
EL	AM	0.0684	0.0388	0.0980	True
EL	QN	−0.0067	−0.0362	0.0229	False
AM	QN	−0.0750	−0.1046	−0.0454	True

The Tukey test is interpreted based on the value of the minimum significant difference (MSD), obtained from the distribution of the studentized amplitude, the mean square of the residues of Anova2, and the sample size of the groups, in the confidence interval determined. For the test, represented in Table 9 and Figure 17, the modulus of the mean difference between the pairs of methods used In the fault's location was greater than the MSD value obtained for the pairs AM—QN, EL—AM, and PRGA—AM. The value 0 (zero) is not contained in the confidence intervals of these pairs, indicating that the average performance is significantly different between them. Furthermore, the percentage errors provided by the AM method were greater than those provided by the three NLO methods.

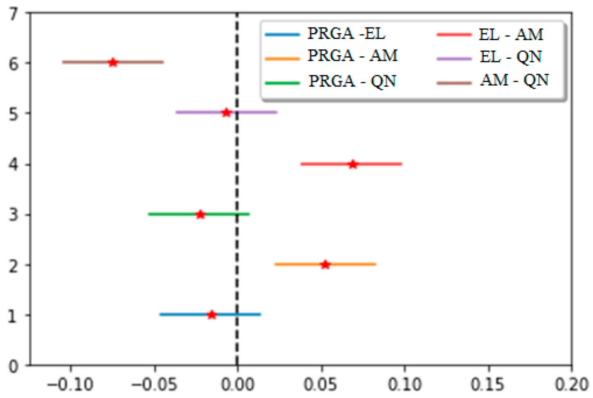

Figure 17. Tukey test: simulated cases.

4.2. Fault Location: Real Cases

The procedures used for the pilot study were applied in other TL. In addition to the 74.4 km transmission line used initially, the techniques for locating faults in three other lines were implemented. Accordingly, the implemented methods were tested in seven real cases of short circuits caused by atmospheric discharge (AD) and fire in the modeled lines, as indicated in Table 11.

Table 11. Characterization: real fault scenarios.

Line	Voltage (kV)	Length (km)	Type	Location (km)	Cause
1	345	74.40	AG BT	60.0 54.0	AD AD
2	500	105.58	AG	30.0	Fire
3	500	342.71	CT AG CT	317.0 76.0 55.0	AD Fire Fire
4	500	248.44	ACT	91.0	AD

The results achieved by the methods for the real cases are recorded in Table 12.

Table 12. Location results: real faults.

Line	Inspection Results (km)	Fault Location (km)				
		ANN	QN	EL	PRGA	AM
1	60 54	55.6 33.5	65.4 54.4	65.4 54.4	65.4 54.4	64.4 54.3
2	30	24.0	23.6	23.6	23.6	29.7
3	317 76 55	306.4 103.0 60.5	311.0 78.4 55.7	311.0 78.4 55.7	311.0 78.4 55.7	324.0 82.7 56.6
4	91	124.0	91.5	91.5	91.5	94.1
Average Error (%)		9.2	2.4	2.4	2.4	1.7
Median Error (%)		6.8	1.2	1.2	1.2	1.4

For the statistical analysis of the results, the location errors were calculated from the difference between the location estimated by the method and the actual distance from the defect (provided by the inspection team) in relation to the length of the line where the bending occurred. For the ANN and the PRGA, the errors were indicated from the average error of the 40 executions.

To identify the existence of differences in the location results that occurred depending on the type of method used, the verification of the randomness, normality, and homoscedasticity supported the assumption that the observations are independent, normally distributed, and maintain the same variance in each treatment, allowing the application of the Anova2 model.

Using the results of the test application presented in Table 13, the null hypothesis of equality between the methods was discarded, and the result of the *p*-value obtained by the test statistic was close to 9.92×10^{-4}, which is considerably less than 5%.

Table 13. Anova2 test: real cases.

	sum_sq	df	F	PR(>F)
C(Type_Fault)	266.130927	6.0	1.239680	0.321484
C(Type_Method)	944.311311	4.0	6.598127	0.000992
Residual	858.708488	24.0	NaN	NaN

Tukey test results presented in Table 14 made it possible to identify a difference in the location of faults performed by the ANN, which provided greater location errors than the other methods.

Table 14. Multiple comparisons of means: Tukey HSD, FWER = 0.05—real cases.

Group1	Group2	Meandiff	Lower	Upper	Reject
PRGA	EL	−1.0258	−10.5193	8.4678	False
PRGA	AM	−1.6714	−11.165	7.8221	False
PRGA	QN	−1.0259	−10.5195	8.4676	False
PRGA	ANN	11.9857	2.4922	21.4793	True
EL	AM	−0.6457	−10.1392	8.8479	False
EL	QN	−0.0001	−9.4937	9.4934	False
EL	ANN	13.0115	3.5179	22.505	True
AM	QN	0.6455	−8.848	10.1391	False
AM	ANN	13.6571	4.1636	23.1507	True
QN	ANN	13.0116	3.5181	22.5052	True

In real cases, using the Tukey test, as shown in Table 14 and Figure 18, there was no statistical evidence identified for the difference between the location of faults carried out between the different optimization methods implemented, nor between these methods and the classic analytical. The module of the mean difference between the pairs of methods used was greater than the value of the MSD obtained for the pairs PRGA—ANN, EL—ANN, AM—ANN, and QN—ANN. The value 0 (zero) is not contained in the interval's confidence of these peers, indicating that average performance is significantly different between them. Furthermore, the worst performance was presented by the ANN.

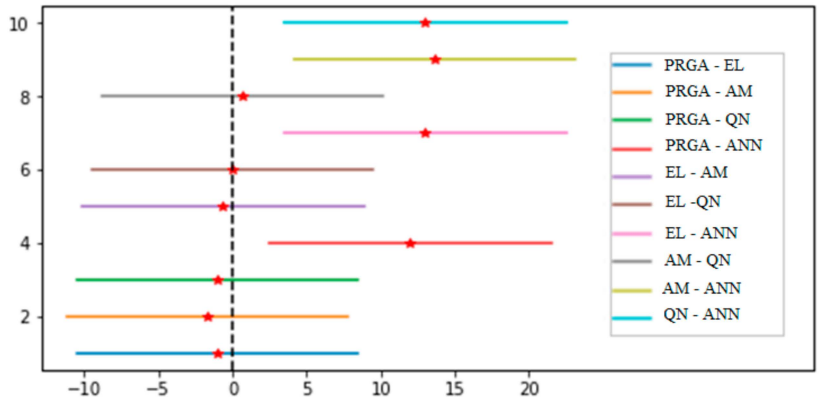

Figure 18. Tukey's test: real cases.

An interesting point to be highlighted for the real cases is that, although the objective functions for the optimization algorithm were developed for the short transmission line model (with only the parameters of resistance and series inductance concentrated), there was no significant difference in the errors obtained in relation to the analytical method, which considers the long-line model. It is noteworthy that only seven cases were investigated (for lines of 74.4 km, 105.58 km, 248.44 km, and 342.71 km), requiring further studies from a larger database. For the cases presented, the short line model used for the transmission line was not preponderant for the results, probably due to other errors such as those caused by current and potential transformer, line parameters, mutual inductance, transposition, and phasor estimation method.

The neural networks, as they have been conventionally used, with voltage and current phasors as input structures, provide reduced errors in simulated cases, but they own the difficulty generalizing for the real fault location function. It should be mentioned that the electrical system model in simulated cases is the same for training and validation, which leads the network to obtain accurate results. The largest errors of the ANN in the real fault location process are related to the values of the Thevenin equivalents (sources and impedance) at the local and remote ends of the transmission line. Electrical systems are dynamic, with load and generation varying 24 h a day. In order to generate the fault files used in the training of location ANN on real cases, the Thevenin voltages and impedances provided by the electric utility were inserted into the ATP, calculated from a short circuit program that considers the static system with light or heavy load. However, the exact values of these equivalents at the time of the fault cannot be determined, which compromises the results of neural networks applied to real cases, contributing to unsatisfactory results. To mitigate the problem, a neural network fault location method, in which the Thevenin equivalents of the line terminals are not needed, is already being developed by the authors. The proposal will enable the practical application of these structures to solve this type of problem in conventional lines and on lines with series compensation, in which fault location becomes more complex due to the non-linearity of the Metal Oxide Varistor, the capacitor's protection element.

5. Conclusions

This study aimed to present and statistically compare applications of artificial neural networks, nonlinear optimization techniques, and a classical analytical method for the problem of fault location in transmission lines in simulated and real scenarios. In the simulated scenarios, the analysis of the percentage errors of the location revealed, with 5% of significance, that the type of method used affects the indication of the location of the short circuit. Smaller errors were observed with neural networks and larger ones with the analytical method, leaving the nonlinear optimization methods with intermediate errors. In real scenarios, unlike the situation verified in simulated environments, there was statistical evidence of higher percentages of errors with neural networks, not rejecting the equality between the location indicated by the analytical method and the nonlinear optimization methods. The neural networks conventionally used for the location function proved incompatible for application in companies that operate electrical systems. No differences were identified among the nonlinear optimization methods. The three methods implemented and applied to the proposed function converged to the expected local minimum. However, it should be noted that the low computational cost and fast response associated with the Quasi-Newton method make it a prominent method. Moreover, the nonlinear optimization methods used for the location function proved to be promising for application in companies that operate electrical systems, providing location errors similar to those presented by the classical analytical method. In this sense, and based on the proposal of this study, it is suggested to consider the application of the methods Quasi-Newton and analytic to improve the answer to the problem of locating faults in transmission lines.

Author Contributions: Conceptualization, S.A.R. and E.G.S.; methodology, S.A.R. and E.G.S.; software, R.T.N.C. and S.A.R.; validation, S.A.R. and E.G.S.; supervision, R.T.N.C. and T.G.M.; writing, S.A.R., E.G.S. and T.G.M. All authors have read and agreed to the published version of the manuscript.

Funding: The APC was funded by Federal Center for Technological Education of Minas Gerais.

Institutional Review Board Statement: Not applicable.

Informed Consent Statement: Not applicable.

Data Availability Statement: Not applicable.

Conflicts of Interest: The authors declare no conflict of interest.

References

1. Chen, Z.; Maun, J.-C. Artificial neural network approach to single-ended fault locator for Transmission Lines. *IEEE Trans. Power Syst.* **2000**, *15*, 370–375. [CrossRef]
2. Joorabian, M. Artificial neural network based fault locator for EHV transmission system. In Proceedings of the 10th Mediterranean Electrotechnical Conference. Information Technology and Electrotechnology for the Mediterranean Countries, Lemesos, Cyprus, 29–31 May 2000; Volume 3, pp. 1003–1006.
3. Mazon, A.J.; Zamora, I.; Gracia, J.; Sagastabeutia, K.J.; Saenz, J.R. Selecting ANN structures to find transmission faults. *IEEE Comput. Appl. Power* **2001**, *14*, 44–48. [CrossRef]
4. Martin, F.; Aguado, J.A. Wavelet-based ANN approach for transmission line protection. *IEEE Trans. Power Deliv.* **2003**, *18*, 1572–1574. [CrossRef]
5. Amorim, H.P.; Huais, L. Faults location in transmission lines through neural networks. In Proceedings of the IEEE/PES Transmision and Distribution Conference and Exposition: Latin America, Sao Paulo, Brazil, 8–11 November 2004; pp. 691–695.
6. Pereira, C.E.M.; Zanetta, L.C. Fault location in transmission lines using one-terminal postfault voltage data. *IEEE Trans. Power Deliv.* **2004**, *19*, 570–575. [CrossRef]
7. Gracia, J.; Mazon, A.J.; Zamora, I. Best ANN structures for fault location in single-and double-circuit transmission lines. *IEEE Trans. Power Deliv.* **2005**, *20*, 2389–2395. [CrossRef]
8. Lin, X.; Mao, P.; Weng, H.; Wang, B.; Bo, Z.Q.; Klimek, A. Study on Fault Location for High Voltage Overhead Transmision Lines Based on Neural Network System. In Proceedings of the International Conference on Intelligent Systems Applications to Power Systems, Kaohsiung, Taiwan, 5–8 November 2007; pp. 1–5.
9. Hagh, M.T.; Razi, K.; Taghizadeh, H. Fault classification and location of power transmission lines using artificial neural network. In Proceedings of the International Power Engineering Conference, Singapore, 3–6 December 2007; pp. 1109–1114.
10. Pereira, C.E.M.; Zanetta, L.C., Jr. An optimization approach for fault location in transmission lines using one terminal data. *Int. J. Electr. Power Energy Syst.* **2007**, *29*, 290–296. [CrossRef]
11. Souza, S.M.; Silva, A.P.A.; Lima, C.S. Voltage and Current Patterns for Fault Location in Transmission Lines. In Proceedings of the International Joint Conference on Neural Networks, Orlando, FL, USA, 12–17 August 2007; pp. 737–742.
12. Ekici, S.; Yildirim, S.; Poyraz, M. A transmission line fault locator based on Elman recurrent networks. *Sci. Direct Appl. Soft Comput.* **2009**, *9*, 341–347. [CrossRef]
13. Ngaopitakkul, A.; Pothisarn, C. Discrete wavelet transform and back-propagation neural networks algorithm for fault location on single-circuit transmission line. In Proceedings of the IEEE International Conference on Robotics and Biomimetics, Guilin China, 19–23 December 2009; pp. 1613–1618.
14. Sahoo, S.; Ray, P.; Panigrahi, B.K.; Senroy, N. A computational intelligence approach for fault location in transmission lines. In Proceedings of the Joint International Conference on Power Electronics, Drives and Energy Systems & 2010 Power India, New Delhi, India, 20–23 December 2010; pp. 1–6.
15. Wei, L.; Guo, W.; Wen, F.; Ledwich, G.; Liao, Z.; Xin, J. Waveform Matching Approach for Fault Diagnosis of a High-Voltage Transmission Line Employing Harmony Search Algorithm. *IET Gener. Transm. Distrib.* **2010**, *4*, 801–809. [CrossRef]
16. Jiang, J.A.; Chuang, C.L.; Wang, Y.C.; Hung, C.H.; Wang, J.Y.; Lee, C.H.; Hsiao, Y.T. A Hybrid Framework for Fault Detection, Classification, and Location—Part I: Concept, Structure, and Methodology. *IEEE Trans. Power Deliv.* **2011**, *26*, 1988–1998. [CrossRef]
17. Lout, K.; Aggarwal, R.K. A feedforward Artificial Neural Network approach to fault classification and location on a 132kV transmission line using current signals only. In Proceedings of the 47th International Universities Power Engineering Conference (UPEC), London, UK, 4–7 September 2012; pp. 1–6.
18. Teklić, L.; Filipović-Grčić, B.; Pavičić, I. Artificial neural network approach for locating faults in power transmission system. *Eurocon* **2013**, 1425–1430.
19. Raoofat, M.; Mahmoodian, A.; Abunasri, A. Fault location in transmission lines using neural network and wavelet transform. In Proceedings of the International Congress on Electric Industry Automation, Shiraz, Iran, 24–25 February 2015; pp. 1–6.

20. Chaitanya, B.K.; Yadav, A.; Andanapalli, K.; Varma, B.R.K. A comparative study of different signal processing techniques for fault location on transmission lines using hybrid Generalized Regression Neural Network. In Proceedings of the 2016 International Conference on Signal Processing, Communication, Power and Embedded System (SCOPES), Odisha, India, 3–5 October 2016; pp. 1246–1250.
21. Ahmed, A.S.; Attia, M.A.; Hamed, N.M.; Abdelaziz, A.Y. Modern optimization algorithms for fault location estimation in power systems. *Eng. Sci. Technol. Int. J.* **2017**, *20*, 1475–1485.
22. Carrión, D.; González, J.W.; IssacI, A.; López, G.J. Optimal fault location in transmission lines using hybrid method. In Proceedings of the IEEE PES Innovative Smart Grid Technologies Conference—Latin America (ISGT Latin America), Quito, Ecuador, 20–22 September 2017; pp. 1–6.
23. Fahim, S.R.; Sarker, Y.; Islam, O.K.; Sarker, S.K.; Ishraque, M.F.; Das, S.K. An intelligent approach of fault classification and localization of a power transmission line. In Proceedings of the IEEE International Conference on Power, Electrical, and Electronics and Industrial Applications, Dhaka, Bangladesh, 29 November–1 December 2019; pp. 53–56.
24. Wang, C.; Yun, Z. Parameter-free fault location algorithm for distribution network T-Type transmission lines. *Energies* **2019**, *12*, 1534. [CrossRef]
25. Elnozahy, A.; Sayed, K.; Bahyeldin, M. Artificial neural network based fault classification and location for transmission lines. In Proceedings of the IEEE Conference on Power Electronics and Renewable Energy, Aswan, Egypt, 23–25 October 2019; pp. 140–144.
26. Onaolapo, A.K.; Pillay Carpanen, R.; Dorrell, D.G.; Ojo, E.E. Transmission line fault classification and location using multi-layer perceptron artificial neural network. In Proceedings of the IECON 2020 The 46th Annual Conference of the IEEE Industrial Electronics Society, Singapore, 18–21 October 2020; pp. 5182–5187.
27. Coban, M.; Tezcan, S.S. Artificial neural network based fault location on 230 kv transmission line using voltage and current signals. In Proceedings of the 4th International Symposium on Multidisciplinary Studies and Innovative Technologies (ISMSIT), Istanbul, Turkey, 22–24 October 2020; pp. 1–4.
28. Kezunovic, M.; Lou, S.; Galijasevic, Z.; Ristanovic, D. Accurate fault location in transmission networks using modeling, simulation and limited field recorded data. *Power Syst. Eng. Res. Cent.* **2002**, 2–44.
29. Ezquerra, J.; Valverde, V.; Mazón, A.J.; Zamora, I.; Zamora, J.J. Field programmable gate array implementation of a fault location system in transmission lines based on artificial neural networks. *IET Gener. Transm. Distrib.* **2011**, *5*, 191–198. [CrossRef]
30. Joorabian, M.; Taleghani, S.M.A.; Aggarwal, R.K. Accurate fault locator for EHV transmission lines based on radial basis function neural networks. *Electr. Power Syst. Res.* **2015**, *71*, 195–202. [CrossRef]
31. Silveira, E.G.; Paula, H.R.; Rocha, S.A.; Pereira, C.S. Hybrid fault diagnosis algorithms for transmission lines. *Electr. Eng.* **2017**, *100*, 1689–1699. [CrossRef]
32. Johns, A.T.; Jamali, S. Accurate fault location technique for power transmission line. *IEEE Proc. C Gener.* **1990**, *137*, 395–402. [CrossRef]
33. Zhang, X.; Pang, B.; Liu, Y.; Liu, S.; Xu, P.; Li, Y.; Xie, Q. Review on detection and analysis of partial discharge along power cables. *Energies* **2021**, *14*, 7692. [CrossRef]
34. Yaacob, M.M.; Alsaedi, M.A.; Rashed, J.R.; Dakhil, A.M.; Atyah, S.F. Review on partial discharge detection techniques related to high voltage power equipment using different sensors. *Photonic Sens.* **2014**, *4*, 325–337. [CrossRef]
35. Birlasekaran, S.; Li, H.J. Detection of faulty insulators on power transmission line. In Proceedings of the 2000 IEEE Power Engineering Society Winter Meeting, Singapore, 23–27 January 2000; Volume 4, pp. 2817–2821.
36. Han, J.; Yang, Z.; Zhang, Q.; Chen, C.; Li, H.; Lai, S.; Hu, G.; Xu, C.; Xu, H.; Wag, D.; et al. A method of insulator faults detection in aerial images for high-voltage transmission lines inspection. *Appl. Sci.* **2019**, *9*, 2009. [CrossRef]
37. Kuwalek, P. AM modulation signal estimation allowing further research on sources of voltage fluctuations. *IEEE Trans. Ind. Electron.* **2019**, *67*, 6937–6945. [CrossRef]
38. Kuwałek, P. Selective identification and localization of voltage fluctuation sources in power grids. *Energies* **2021**, *14*, 6585. [CrossRef]
39. Taqi, A.; Beryozkina, S. Overhead transmission line thermographic inspection using a drone. In Proceedings of the IEEE 10th GCC Conference & Exhibition (GCC), Kuwait, Kuwait, 19–23 April 2019; pp. 1–6.
40. EMTP Center. *Alternative Transients Program Rule Book*; EMTP Center: Leuven, Belgium, 1990.
41. Yu, T.C.; Martí, J.R. A robust phase-coordinates frequency-dependent underground cable model (zCable) for the EMTP. *IEEE Trans. Power Deliv.* **2003**, *18*, 189–194. [CrossRef]
42. Marti, L. Simulation of transients in underground cables with frequency-dependent modal transformation matrices. *IEEE Trans. Power Deliv.* **1988**, *3*, 1099–1110. [CrossRef]
43. Coury, D.V.; Oleskovicz, M.; Aggarwal, R.K. An ANN routine for fault detection, classification and location in transmission lines. *Electr. Power Compon. Syst.* **2002**, *30*, 1137–1149. [CrossRef]
44. Santos, A.; Gaspar, C.; Barros, M.T.C.; Duarte, P. Transmission line fault resistance values based on field data. *IEEE Trans. Power Deliv.* **2020**, *35*, 1321–1329. [CrossRef]
45. Andrade, V.D.; Sorrentino, E. Typical expected values of the fault resistance in power systems. In Proceedings of the IEEE/PES Transmission and Distribution Conference and Exposition: Latin America, Sao Paulo, Brazil, 8–10 November 2010; pp. 602–609.
46. Phadke, A.G.; Thorp, J.S. *Computer Relaying for Power Systems*; John Wiley & Sons Inc.: Hoboken, NJ, USA, 1998; p. 289.
47. Demuth, H.; Beale, M. *Neural Network Toolbox User'S Guide*; The MathWork: Natick, MA, USA, 2015.

48. Luenberger, D.G.; Ye, Y. *Linear and Nonlinear Programming*; Springer: Berlin/Heidelberg, Germany, 2008.
49. Bland, R.G.; Goldfarb, D.; Todd, M.J. Feature Article—The ellipsoid method: A survey. *Inst. Oper. Res. Manag. Sci.* **1981**, *29*, 1039–1091. [CrossRef]
50. Takahashi, R.H.C.; Vasconcelos, J.A.; Ramirez, J.A.; Krahenbuhl, L. A multiobjective methodology for evaluating genetic operators. *IEEE Trans. Magn.* **2003**, *39*, 1321–1324. [CrossRef]
51. Python Software Foudation. Python Language Site: Documentation. 2022. Available online: https://www.python.org/psf/ (accessed on 7 January 2022).
52. Montgomery, D.C.; Runger, G.C. *Applied Statistics and Probability for Engineers*; John Wiley & Sons: Hoboken, NJ, USA, 2014.
53. Montgomery, D.C.; Peck, E.A.; Vining, G.G. *Introduction to Linear Regression Analysis*; John Wiley & Sons: Hoboken, NJ, USA, 2021.